

High Resolution Oxygen Isotope Stratigraphy for the Last 150,000 Years in the Southern South China Sea: Core MD972151

Meng-Yang Lee¹, Kuo-Yen Wei¹, Yue-Gau Chen¹

(Manuscript received 18 November 1998, in final form 19 January 1999)

ABSTRACT

A detailed high-resolution oxygen isotope stratigraphy over the last two glacial-interglacial cycles in the southern South China Sea is presented, based upon analysis of *Globigerinoides sacculifer* (planktic foraminifera) in Core MD972151. Major characteristic isotopic events were identified and correlated to the standard SPECMAP chronology. In addition, radiocarbon dating and a few biostratigraphic, geomagnetic and tephrochronologic markers were employed to enhance the reliability and resolution of the age model. The tephra layer of the Toba Eruption at 71 ka helps to anchor the boundary of Stages 5/4, and provides a yardstick correlating to the cold period between interstadials 19 and 20 identified in the GISP2 Greenland ice core. The last appearance of pink *Globigerinoides ruber* and the Blake magnetic polarity event in the lower part of the core helped us to locate the transition of Stage 6/5e. Our high-resolution oxygen isotope stratigraphy, however, indicates that the age of the Blake magnetic reversal occurred during the Stage 6/5e transition instead after the warmth peak of the isotopic event 5e.

The resulting age model shows that the 26.54 m sequence from Core MD972151 provides a continuous record from 153 to 0.94 ka, with sedimentation rates varying between 5.6 and 78 cm/kyr. The temporal resolution of the isotopic record is about 60 -150 years per sample for the upper part of the core and 250 years for the lower part, respectively.

(Key words: South China Sea, Oxygen isotope, Late Quaternary, Chronology)

1. INTRODUCTION

Distinguished by its warmest mean annual sea surface temperature (> 28°C) on the earth, the western Pacific warm pool (WPWP) responds to the strengths of both the Walker and the Hadley circulations (Wyrki, 1981) and provides the atmosphere with a vitally large amount of latent heat and water vapor. With active exchanging with warm equatorial waters through the

¹Department of Geology, National Taiwan University, 245 Choushan Road, Taipei, Taiwan, ROC

Sunda Shelf and adjacent straits, the southern South China Sea (SCS) maintains annual average sea surface temperatures (SSTs) of above 28°C. As it occupies the western extent of the WPWP, the southern part of the South China Sea is unique in experiencing seasonal reversal East Asia monsoons. Reconstruction of the variability of the southern South China Sea during glacial-interglacial oscillations will be essential for evaluating its role in influencing the WPWP and the East Asia monsoon climates. For any sedimentary sequence to be studied for this purpose, it is imperative to obtain a reliable oxygen isotope stratigraphy as the first step in establishing a chronological framework.

Although a standard chronology based upon stacked oxygen isotope records of foraminifera from deep-sea sediments of the late Quaternary has been available for more than a decade (Imbrie et al., 1984; Prell et al., 1986; Martinson et al., 1987), a truly high resolution oxygen isotopic stratigraphy over the last two glacial-interglacial cycles has not been obtained for the South China Sea. Limited by the penetration depth of piston coring, cores which record the last interglacial period are inevitably those with low sedimentation rates and therefore low resolution. The resolution for most available records of this area is roughly several thousand years per sample (Wang et al., 1986; Wang and Chen, 1990, Wang and Wang, 1990; Schonfeld and Kudrass, 1993), except for a high-resolution record obtained from the Sulu Sea which took advantage of the sufficient length of the ODP Site 769 (Linsley, 1996). On the other hand, high-resolution paleoceanographic studies have been carried out only for the last glacial and the Holocene (e.g., Thunell and Maio, 1996; Huang et al., 1997a, 1997b; Wei et al., 1998). There is virtually no high-resolution record for the past few glacial-interglacial cycles in the South China Sea.

During Leg II of the IMAGES III Cruise in June 1997, around the SCS, ten long, giant piston cores were obtained (Chen et al., 1998). Among them, Core MD972151, measuring 2672 cm in length, was raised from the northern slope of the Wan-An Shallow (8° 43.73'N, 109°52.17'E) off southeastern Vietnam at a water depth of 1550 m (Figure 1). On-board preliminary examination revealed that the bottom of the core was slightly earlier than the last appearance of the pink-pigmented form of *Globigerinoides ruber*, and therefore promised a record of possibly high-resolution (153 kyr/2672cm = ~60 years per cm). The combination of high temporal resolution, high carbonate content (5~25%) (Huang et al, this volume), excellent paleomagnetic record (Lee et al., this volume), and good preservation of calcareous microfossils, makes this core the first of such superb quality to be obtained from the southern South China Sea. We have then chosen this core as our first target site for establishing a long, high-resolution oxygen isotope stratigraphy for the southern South China Sea. This paper reports the oxygen isotopic analysis results and the corresponding detailed chronology for Core MD972151.

2. MATERIAL AND METHOD

The cored sequence consists mainly of dark gray hemipelagic muds. No turbidites or volcanic layers were detected visually. Samples were taken every 4 cm down to 2400 cm and then every 8 cm down the lower section to the bottom. In compensating a void of 22.5 cm in

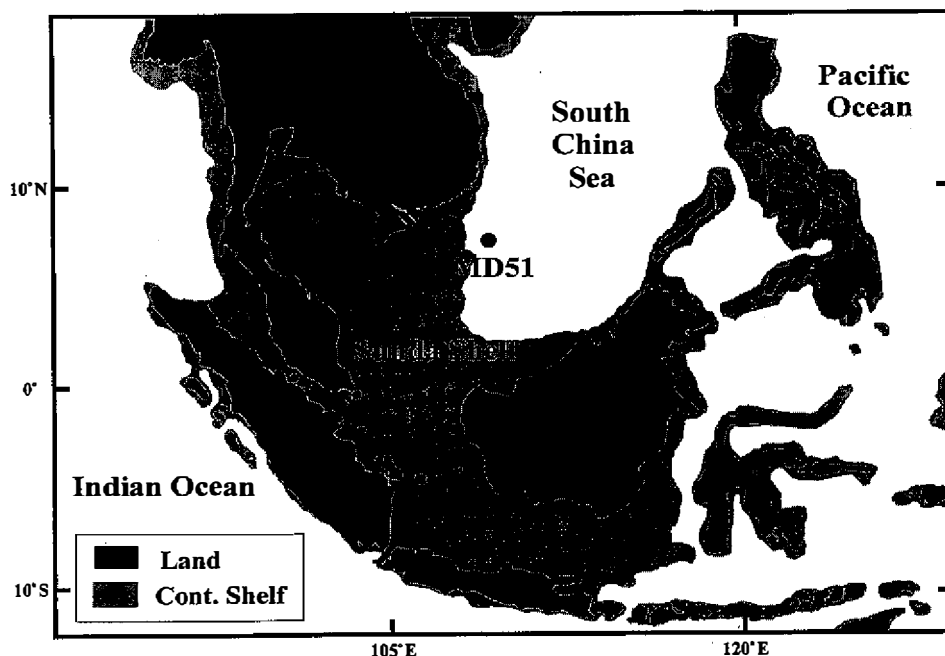


Fig. 1. Map showing the location of the studied Core MD972151 in the southern South China Sea. The 100-m bathymetric isoline delineates the continental shelf (gray area) which is submerged at present, but emerged as land during the last glacial maximum.

length in the interval between 1107.5 cm and 1130 cm, depths below 1130 cm were converted into new values by subtracting 22.5 cm from their original recorded readings.

Specimens of a surface-dwelling planktonic foraminifera species, *Globigerinoides sacculifer*, were picked from the 300-350 μm size fraction. The reason to restrict the size range of specimens within a narrow size fraction was to minimize possible vital effects associated with test size (Berger et al., 1978). The picked specimens were cleaned by ultrasonic vibration for 10-15 seconds twice to remove adhering fine particles. Samples were then treated with NaClO (5%) at room temperature for 24 hours to remove organic matter. Isotope measurements were performed on a Finnegan Delta Plus mass spectrometer with a Kiel automated carbonate device at the Department of Geology, National Taiwan University. For each analysis, six foraminiferal specimens were used. The cleaned foraminiferal tests were interreacted with 100 % phosphoric acid at 70°C. Analyses were duplicated or triplicated for every sample. The average difference between individual analyses for each sample was about 0.26 ‰ for oxygen and 0.18 ‰ for carbon. A difference of 0.5 ‰ between analyses was used as the upper tolerant value to detect possible deviant measurements among the multiple analyses. Average values from the screened duplicated or triplicated results were then calculated and reported with respect to the PDB standard through calibration against the routinely analyzed NBS 19

standard ($\delta^{18}\text{O}_{\text{PDB}} = -2.20\text{‰}$ and $\delta^{13}\text{C}_{\text{PDB}} = +1.95\text{‰}$) with a precision of 0.08‰ for oxygen and 0.04‰ for carbon.

To date the topmost part of the core, planktic foraminiferal specimens from 12 strategically selected levels were radiocarbon dated. For each level, more than 150 specimens of *G. sacculifer*, weighing about 4-6 mg, were picked, cleaned and then converted to CO_2 gas for accelerator mass spectrometry (AMS) ^{14}C dating at the Institute of Nuclear and Geological Sciences, New Zealand. The oxygen isotope data of core MD972151 are available electronically at the Paleooceanographic Data Center of Core Laboratory - Center for Ocean Research, NSC, at the Institute of Applied Geophysics, National Taiwan Ocean University, Keelung, Taiwan, R.O.C. (Internet: <http://140.121.175.114>).

3. OXYGEN ISOTOPE STRATIGRAPHY AND CHRONOLOGY

AMS ^{14}C dating and oxygen isotope stratigraphy formed the major basis for our chronologic correlation for Core MD972151. Additional age markers, such as the last appearance datum of pink variant of *Globigerinoides ruber* and the Blake magnetic polarity event, were also used to help in identifying the oxygen isotope Stage 6/5e transition (Figure 2). The merits of each of these stratigraphic and chronologic markers are described as follows.

The AMS ^{14}C dates obtained from 12 intervals are listed in Table 1. It has been demonstrated that in the southern South China Sea there is a significant difference in radiocarbon age, roughly 700 years, between shallow-dwelling and deep-dwelling planktic foraminifera for the same stratigraphic level (e.g., in a near-by site, V35-5, Broecker et al., 1988a). To obtain high-resolution radiocarbon dating, we selected only *G. sacculifer* for AMS radiocarbon dating to rule out possible bias. The resulting radiocarbon ages were first corrected by subtracting 400 years for the reservoir effect (Bard, 1988), then the corrected ages were further converted to calendar years using the revised CALIB 3.0 Program (Stuiver and Reimer, 1993). For instance, the oldest dated radiocarbon age, 15626 yr. BP, has been converted to a calendar age of 18147 yr. BP (see Table 1).

For the lower part of the core (older than 20 ka), chronological correlation was based on mainly oxygen isotope stratigraphy. To offset the high-frequency variation, the original time-series was smoothed using a 5-point moving average as shown in Figure 2. Various oxygen isotopic events (Table 2) were identified by correlating the resulting smoothed $\delta^{18}\text{O}$ time-series with the standard composite $\delta^{18}\text{O}$ record of the SPECMAP (Pisias et al., 1984; Prell et al., 1986). Most of the second-order isotopic events were identifiable. As the amplitude of planktic $\delta^{18}\text{O}$ fluctuations within Stage 5 was relatively small compared to that in the SPECMAP record, we also referred to the $\delta^{18}\text{O}$ curve of coexisting benthic foraminifera (Van, V.-T., unpublished data) to corroborate the identified $\delta^{18}\text{O}$ events. The assigned dates for the identified $\delta^{18}\text{O}$ events were adopted from the high resolution chronostratigraphy of Martinson et al. (1987).

3.1. Tephra of Toba Eruption

The interval at subdepth 1558 cm contains abundant coarse glass shards, as manifested by

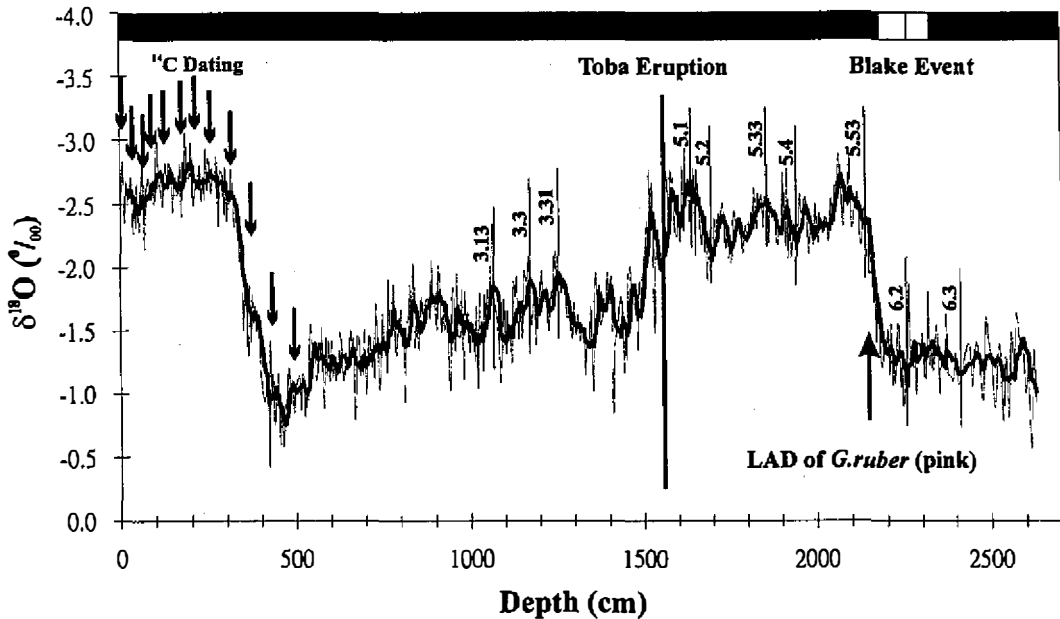


Fig. 2. Time-series of $\delta^{18}\text{O}$ of surface-dwelling planktic foraminifera *G. sacculifer* from MD972151, plotted against depth in core. Vertical arrows mark AMS radiocarbon dates shown in Table 1. Digital numbers represent various oxygen isotopic events correlated to the standard marine isotopic record of SPECMAP stack (Table 2). The upper bar shows the magnetic polarity pattern. The Black Event is characterized by two reversals (white) and a short normal interval (black) in between. The large arrow marks the last appearance datum of the pink variant of *G. ruber* at subdepth 2149 cm. The bold vertical line indicates the interval of Toba glass shards.

the highest peak abundance of coarse grains ($>63\ \mu\text{m}$) throughout the core (Figure 3). These glass shards were identified to be tephra deposited from the Toba eruption of Sumatra (Chen, C.-H., pers. comm., 1999). The super-eruption of Toba in Sumatra, occurring during the stage 5a-4 transition of the marine oxygen isotopic record (Ninkovich et al., 1978), was the largest explosive eruption in magnitude that has been documented for the late Quaternary. Owing to the prevailing stratospheric jet streams, the Toba ash was dispersed mainly to the west-north-west, more than 4000 km from the source. Particles have been traced from Malaysia to the Bay of Bengal and up to the southeastern Arabian Sea (Ninkovich et al., 1978; Rose and Chesner, 1987; Schulz et al., 1998), covering at least 1 % of the Earth's surface with an extensive ash blanket.

Several lines of reasoning have led us to the conclusion that the glass shards found at the 1558 cm interval were deposited from the Toba eruption. First of all, this interval was slightly later than the oxygen isotopic event 5.1 (79.25 ka) but much earlier than event 3.31 (55.45 ka) (Martinson et al., 1987). More precisely, this level is in the transition interval from event 5.1 to

Table 1. Ages derived from the accelerator mass spectrometer ^{14}C measurement of planktic foraminifera for twelve samples in Core MD972151.

Depth in core (cm)	AMS ^{14}C age (^{14}C yr. BP)	Calendar [#] age (cal. yr. BP)
3-4	1437 \pm 66	938
35-36	1897 \pm 56	1353
71-72	2575 \pm 56	2143
91-92	2986 \pm 67	2743
127-128	3869 \pm 65	3697
171-172	4404 \pm 57	4499
211-212	5323 \pm 67	5648
251-252	6810 \pm 66	7276
311-312	9329 \pm 72	9927
371-372	11846 \pm 78	13359
423-424	13071 \pm 80	14907
495-496	15626 \pm 87	18147

AMS ^{14}C ages were calibrated through the revised Calib 3.0 program

(Stuiver and Reimer, 1993) after subtracting a global-average surface ocean reservoir effect by 400 yr. (Bard et al., 1988).

event 4.22 (64.09 ka). This age interval falls within the range of radiometric dates of the Toba deposits, 73,000 to 75,000 yr. BP (Ninkovich et al., 1978; Chesner et al., 1991), or the ice-core dated age of the same event, 71,000 \pm 5000 yr. BP (Zielinski et al., 1996). This temporal coincidence led us to infer that the glass shards are indeed tephras of the Toba eruption. Secondly, oxygen isotopic record of MD972151 shows a significant positive excursion (>0.6 ‰) immediately above the ash layer, indicating a substantial cooling. This phenomenon fits the detected climatic variation immediately after the Toba eruption, shown in the high-resolution paleoclimatic record of the GISP2 Greenland ice core: after the eruption, a pronounced cooling of 1000 years set in, which ended the warm period of the interstadial (IS) 20 (Zielinski et al., 1996). Finally, sediments at depth 1558cm consist mainly of glass shards and, at the same, do not show any increase in magnetic susceptibility (Chen et al., 1998; Lee T.-Q., this volume). This high abundance of glass shards and low content of magnetic minerals (inferred from the low magnetic susceptibility) indicates that the geochemical character of the tephras is comparable to that of Toba tephras, composed dominantly of rhyolitic bubble-wall glass shards (Rose and Chesner, 1987).

Table 2. List of age controlling points identified by correlating oxygen isotopic events in MD972151 with SPECMAP stack (Martinson et al., 1987) augmented by an additional tephrochronological mark of Toba Ash (Zielinski et al., 1996).

Event	SPECMAP age (cal. yr. BP)	Depth in core (cm)
3.13	43880 ± 4710	1061
3.3	50210 ± 3850	1168
3.31	55450 ± 5030	1241
Toba Eruption	71000 ± 5000	1558
5.1	79250 ± 3580	1620
5.2	90950 ± 6830	1685
5.33	103290 ± 3410	1860
5.4	110790 ± 6280	1950
5.53	125190 ± 2920	2133
6.2	135100 ± 4240	2240
6.3	142280 ± 5280	2406

For the age of the Toba eruption, we here adopted the date inferred from the GISP 2 ice core: 71,000 years BP (Zielinski et al., 1996). The Toba eruption, therefore, provides an isochronous stratigraphic horizon to correlate with the Greenland ice core record.

3.2. Last Appearance Datum of Pink *Globigerinoides Ruber*

Pink variants of *Globigerinoides ruber* occur persistently in sections below 2149 cm, validating the last appearance datum (LAD) of this form as a reliable marker for the oxygen 5e/6 transition throughout the Indo-Pacific area (Thompson et al., 1979; Cang et al., 1988; Wang and Wang, 1990; Schonfeld and Kudrass, 1993). Thompson et al. (1979) assert that the true level for the top of the range of pink *G. ruber* is probably after the 6/5e transition but before the 5d interglacial stadium. Nevertheless, a closer examination of the results of Thompson et al. (1979) reveals that the higher the sedimentation rate, the older the LAD of pink *G. ruber*, for most of the 10 studied deep-sea cores from the Pacific and Indian Oceans. For example, three cores with average sedimentation rates higher than 5 cm/kyr showed that the pink variant of *G. ruber* lasted through Stage 6 to the beginning of Stage 5, whereas others with lower sedimentation rates showed it lasted up to the close of Stage 5e. The apparent diachronous disappearance of pink *G. ruber* is believed to be an artifact caused by bioturbation.

The high sedimentation rate of Core MD972151 allows us to further pinpoint the age of the LAD of pink *G. ruber* at 127 ka, instead of 120 ka.

3.3. Magnetic Blake Event

The directions of the stable remanent magnetisation show an anomalous zone at depths between 2170 and 2380cm, exhibiting two short reversed intervals separated by a short normal interval (Lee, T.-Q., pers. comm., 1999). A similar pattern associated with the Blake polarity event dated around 117 ka in various marine cores and loess deposits has been identified (Tucholka et al., 1987; Tric et al., 1991; Fang et al., 1997). In Core MD 972151, this geomagnetic polarity event occurs during the transition from oxygen isotope Stage 6 to 5e (Figure 2), corresponding to the interval between 128.5 ka and 141.1 ka, with a duration of 12.6 kyr. This age assignment, however, is 11 kyr earlier than the dates determined by previous studies (Tucholka et al., 1987; Tric et al., 1991; Fang et al., 1997). This obvious discrepancy in age determination, one being older than event 5e while the other younger, remains an

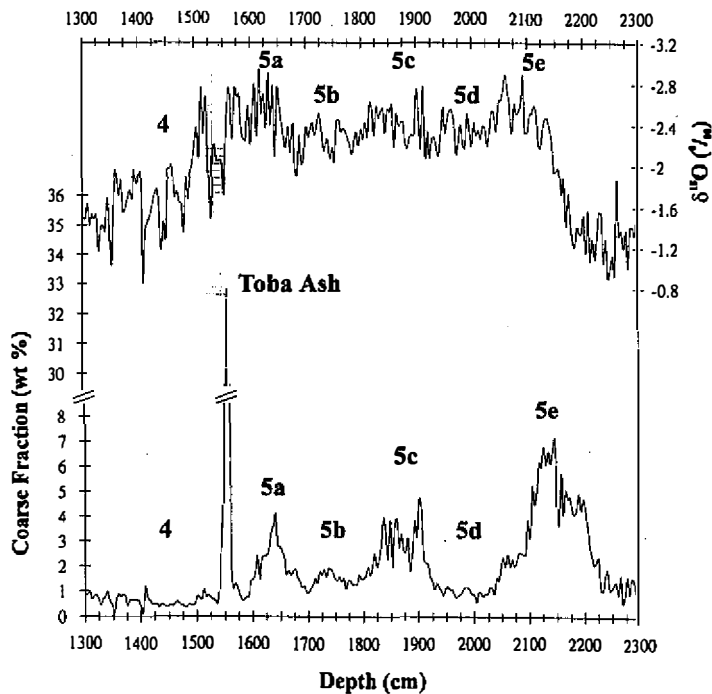


Fig. 3. Position of Toba tephra in the oxygen isotope stratigraphy of MD 972151. Upper panel: $\delta^{18}\text{O}$ vs. depth of core MD972151 between 1300 cm and 2300 cm. The stippled area marks the cooling period following the Toba eruption. Lower panel: Coarse fraction ($>63 \mu\text{m}$) abundance vs. depth. A peak abundance of coarse fraction composed mainly of glass shards occurs at subdepth 1558cm.

enigma at present. Geomagnetic polarity reversals should occur simultaneously worldwide, and thus provide a synchronous marker useful for correlating terrestrial and marine records. The earlier date (by 10-15 kyr) registered for the Blake polarity event in Core MD972151 in the southern SCS implies that the depth of magnetic remanence acquisition was somewhat deeper at this site compared to other sites. Judging from the sedimentation rates above the Black episode, we suggest that the depth of remanence acquisition was at about 100 - 150 cm below the water-sediment interface. This estimation, however, is about one order larger than what was previously suggested (DeMenocal et al., 1990; Tauxe et al., 1996).

In summary, the chronology of Core MD972151 is mainly based upon radiocarbon dating for the uppermost part and planktic foraminiferal oxygen isotope stratigraphy for the rest of the core. Three additional markers were augmented to further constrain the age assignments: (1) the glass shards at subdepth 1558 cm, correlating to the Toba eruption event at 71 ka; (2) the last appearance datum of pink variant of *G. ruber* at subdepth 2149 cm, marking the transition of stage 6/5e; and (3) the geomagnetic Black Event at subdepth 2170- 2380 cm, as a marker near the boundary of stage 6/5e. This newly established chronology, with its high resolution, indicates that the ages for the last two markers can be slightly modified.

4. SEDIMENTATION RATES

Figure 4 shows the age and depth relationships established for Core MD972151. By extrapolation, the core-top is dated at 0.94 ka whereas the base is 153 ka. The interval of the upper Holocene has the highest sedimentation rates, ranging from 24 to 78 cm/kyr, with an average value of 32 cm/kyr. The apparent high sedimentation, however, is partially an artifact caused by extension of the uppermost part of the core due to sucking pressure exerted during piston coring, and partially due to the high water content of the section. The sedimentation rates decrease to about 14 - 23 cm/kyr and remain relatively stable down to the bottom except for the intervals of Stage 5 where sedimentation rates are the lowermost, ranging from 5.6 to 14.2 cm/kyr. The temporal resolution for the Holocene is about 60-150 years per sample while that for the lower part of the core is about 250 years per sample.

Previous compilations of sedimentation rates in the SCS showed an increase of accumulation rates for glacial periods by a factor of 2 to 5 as compared to those for interglacial periods (Schonfeld and Kudrass, 1993; Wang et al., 1995). This phenomenon was attributed to the enhanced input of terrigenous sediments into the South China Sea basin during glacial times (Broecker et al., 1988b; Wang and Wang, 1990; Schonfeld and Kudrass, 1993; Wang et al., 1995). In other words, during high stands of sea level, most riverine input sediments load upon continental shelf and only a small amount is transported to the continental slope. The change of sedimentation rates on the continental slope, such as at the site of MD972151, mainly reflect the changing deposition loci of terrigenous input governed mainly by rise and fall of sea level. Site MD972151, located on the northern side of the Wan-An-Shallow, under the lee side of sedimentation fluxed from the Sunda Shelf, shows moderate change in sedimentation rate in the glacial-interglacial cycles. The sedimentation rates of Stages 6 and 2-4 (glacial time) are only 2 - 3 fold of that of Stage 5 (Figure 4). We speculate that, during the glacial time when a

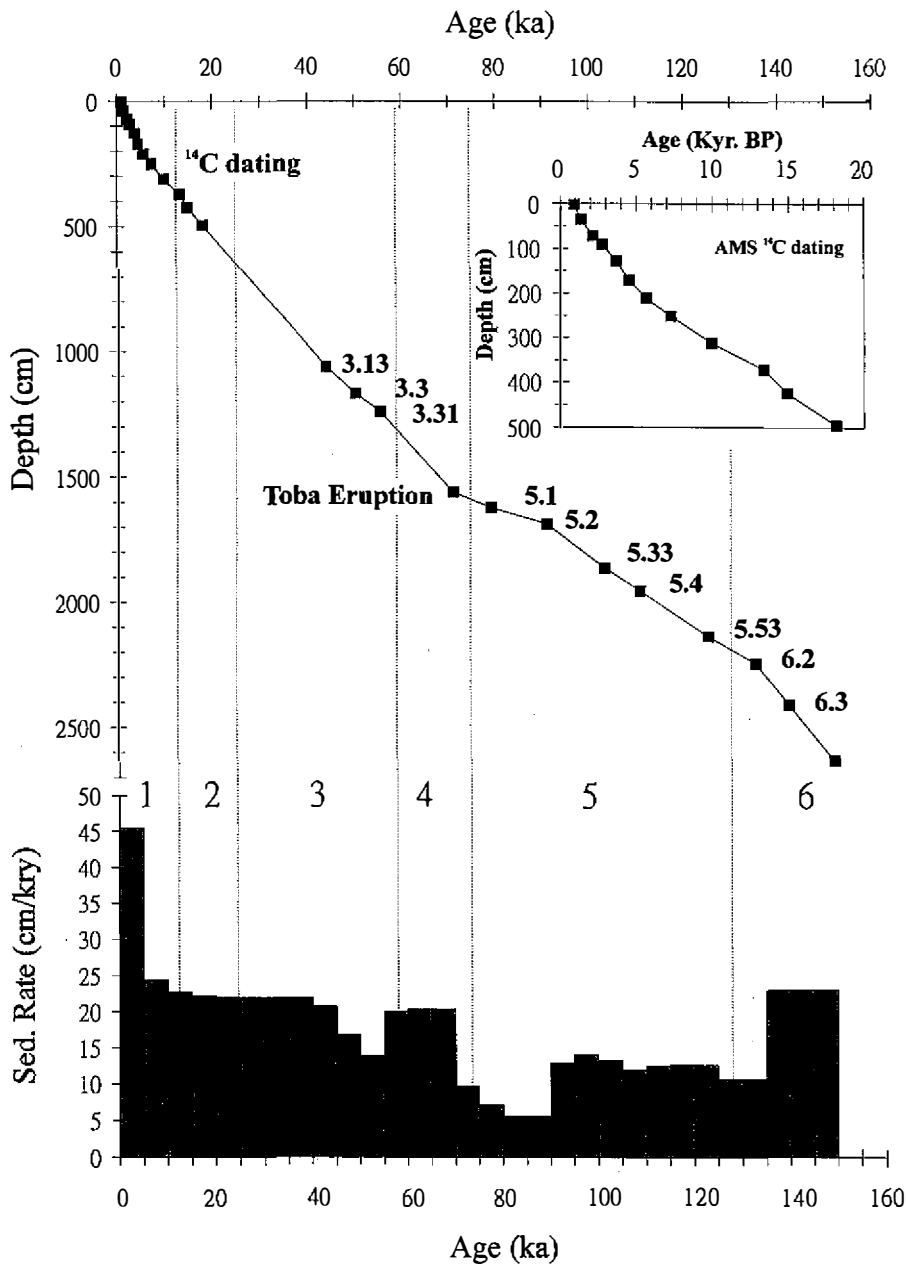


Fig. 4. Age-depth model and corresponding sedimentation rate variation. Upper panel: Plot of depth against chronological controlling points obtained from AMS ¹⁴C dating, oxygen isotopic events and Toba ash. Inserted plot shows the twelve AMS ¹⁴C dates against depth. Lower panel: Histogram of sedimentation rates of Core MD972151 calculated every 5000 yrs.

large portion of the Sunda Shelf was exposed, only fine particles of the distal part of the terrigenous sediments were deposited at this site, but not those transported by down-slope gravity currents.

5. DISCUSSION

The oxygen isotopic record provided by Core MD972151 is the most detailed for the South China Sea over the last two glacial-interglacial cycles (Figure 5). Over the past 150 kyr, the $\delta^{18}\text{O}$ values fluctuated from -3.1‰ to -0.4‰. The $\delta^{18}\text{O}$ values in the uppermost section are more depleted relative to those documented by northern South China Sea cores (Wang and Wang, 1990; Huang et al., 1997a, 1997b; Wei et al., 1998). As also shown in other cores from the southern South China Sea (Wang et al., 1986; Wang and Chen, 1990; Duplessy et al., 1991; Schonfeld and Kudrass, 1993; Miao et al., 1994), these light values reflect a condition of higher temperature and/or lower salinity of surface waters compared to the northern part of the SCS.

The decrease in $\delta^{18}\text{O}$ during Termination I and Termination II is 2.4‰ and 2‰, respectively, comparable to the amplitude observed between the last glacial maximum and the Holocene from a near-by core V35-5 (Duplessy et al., 1991). By subtracting the ice volume effect of 1.2‰ (Fairbanks, 1989) from the last-glacial-interglacial difference, the average temperature difference between the last glacial maximum (LGM) and the Holocene for the surface water is estimated to be 4~5°C (ignoring salinity effects). This estimation is comparable with previous micropaleontological analyses for the southern SCS that during the LGM the winter SSTs were about 22°C and summer SSTs about 28°C (Miao et al., 1994; Wang et al., 1995; Thunell and Miao, 1996).

In comparison to the SPECMAP stack (Martinson et al., 1987), our oxygen isotopic curve shows some characteristic features pertinent to the southern South China Sea. Firstly, the planktic $\delta^{18}\text{O}$ difference between the two major interstadials (Stages 5a, 5c) and the last interglacial peak (Stage 5e) is less pronounced, resulting in a plateau-like pattern for Stage 5 (Figure 5). This implies that salinity in the southern SCS during Stage 5 might be significantly different from the present. Secondly, superimposed on the general variation of glacial-to-interglacial changes, there are frequent short-term $\delta^{18}\text{O}$ fluctuations during Stages 2, 3 and 4. These events can be correlated to the millennial variation of $\delta^{18}\text{O}$ in the GISP2 ice core of Greenland (Dansgaard et al., 1993; Meese et al., 1994) (Figure 6). These two particular features are further discussed below.

5.1. Oxygen Isotopic Stage 5

At present, the average depth of the Sunda Shelf is about 40m. For the intervals 75-110 ka, the sea level changes derived from raised coral reef terraces and from oxygen isotopes in deep sea cores were within the range of -20 to -60m relative to the present sea level (Chappell and Shackleton, 1986; Shackleton, 1987; Chappell et al. 1996). More precisely, sea level held at about -20m relative to the present during Stage 5a and Stage 5c, but fell to about -62m and -44m during Stage 5b and Stage 5d, respectively. The exposure of the Sunda Shelf is rather

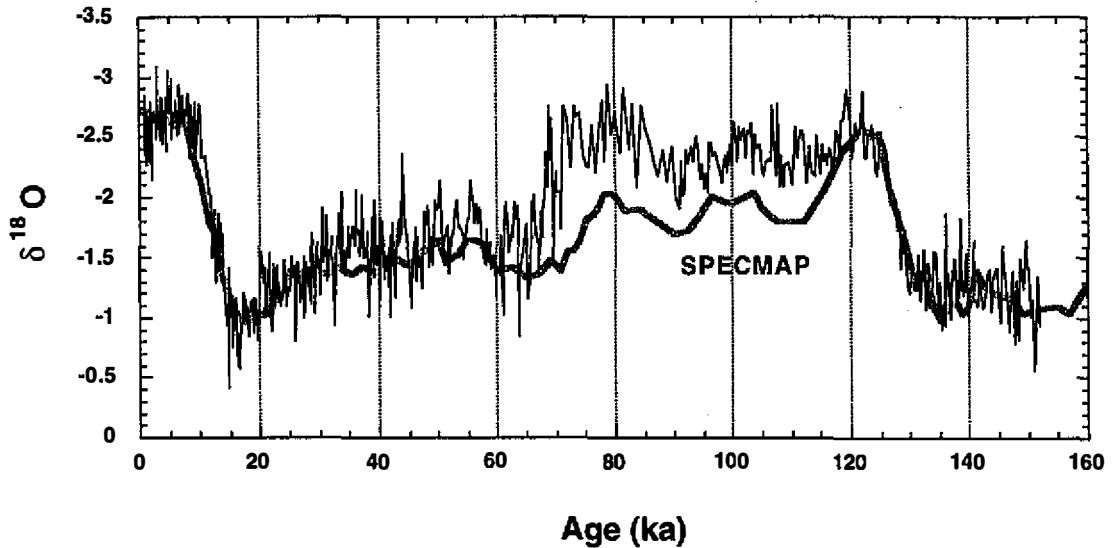


Fig. 5. Time series of $\delta^{18}\text{O}$ of *G. sacculifer* (fine curve) superimposed upon the SPECMAP stack (bold curve) for the past 160 kyr..

sensitive to the rise and fall of sea level with a critical depth of 30-40m. As the WPWP remained relatively warm and stable during the late Quaternary (Broecker, 1986; Thunell et al., 1994; Ohkouchi et al., 1994; Linsley, 1996), the planktic foraminifera at Core MD972151 would record the $\delta^{18}\text{O}$ signal of the northward flow of warm equatorial waters when the sea level was high in Stage 5e. During Stages 5d to 5a, sea surface temperatures might have dropped a little, and so did the sea level. Although the fall of sea level was slight, it was sufficient to cut off the through flow and leave the southern SCS isolated from the open oceans. The site of MD972151 was then under a stronger influence of regional hydrological and precipitation conditions. The relatively light values of $\delta^{18}\text{O}$ for most of Stage 5 (i.e., from Stages 5d to 5a, 110 to 70 ka) indicate a lower salinity condition than that of the open oceans. This indicates that, during this period, the precipitation over the southern SCS and probably Indochina was relatively high.

5.2. Oxygen Isotopic Stages 2-4

Usually, it is hard to tie the oxygen isotopic stages 3 and 4 to a definite chronology. As discussed in the preceding section, with the constraints put by the Toba tephra at 71 ka and radiocarbon dating in Stage 2, Stages 3 and 4 are easily bracketed. The cooling immediately following the Toba eruption shown in Core MD972151 provides a link to the cooling period sandwiched between the interstadials 19 and 20 in the ice core record of GISP2 (Figure 2). Based upon the chronological framework thus obtained, the peaks and valleys in the MD 972151 $\delta^{18}\text{O}$ time-series can be correlated, one by one, to that in the GISP2 record (Figure 6). The six Heinrich events recognized in the northern Atlantic Ocean (e.g., Bond et al., 1993) can also be correlated to positive excursions in the MD972151 record. Although the correlation is

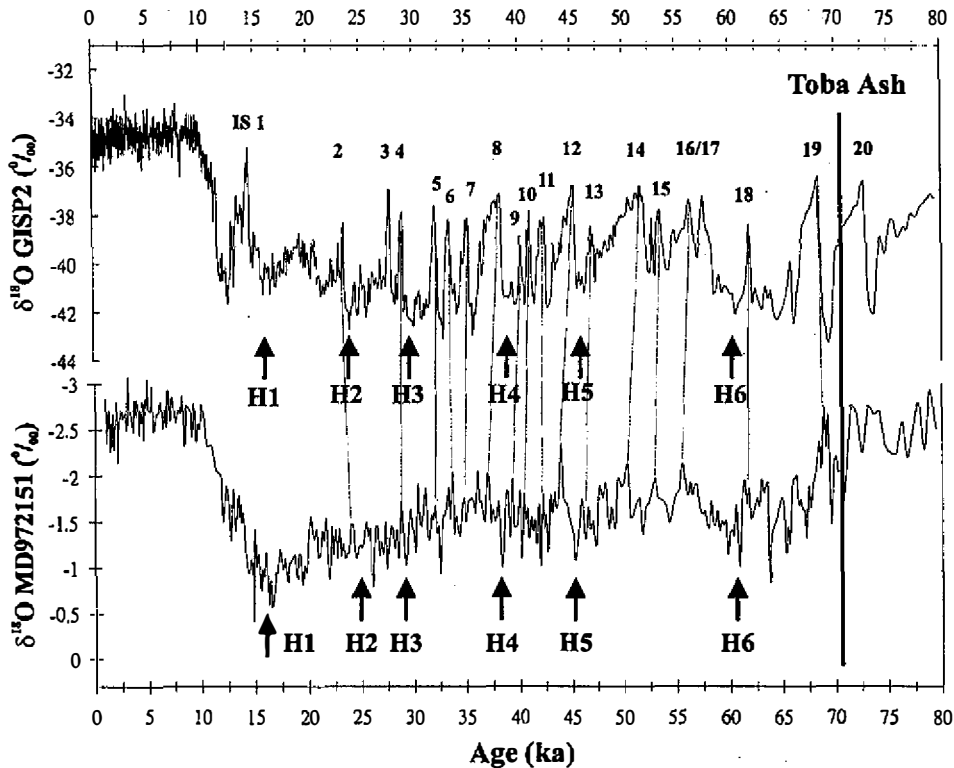


Fig. 6. Correlation of high-frequency fluctuation in the $\delta^{18}\text{O}$ of the Greenland GISP2 ice core with the $\delta^{18}\text{O}$ record of Core MD972151 for the past 80 ka.

tentative, the high-frequency variations in the $\delta^{18}\text{O}$ record do suggest that there is a teleconnection between Greenland and the southern SCS in terms of tempo and mechanism of paleoclimatic changes, such as through the modulation of atmospheric vapor content (Schulz, 1998; Broecker, 1997). The lead and lag relationships of various proxies between these two geographically remote areas warrant further investigation.

Acknowledgements This study is a contribution to the Taiwan IMAGES Program. The participation of MYL and KYW in the IMAGES-IPHIS Curise during 1997 was funded by the National Science Council under Grants NSC86-2611-M-002-006 and NSC86-2111-M-019-005. The support offered by French MENRT, TAAF, CNRS/INSU and IFRTP to the operation of the curise vessel Marion Dufresne and the IMAGES Program is highly appreciated. This research was supported by Grant NSC87-2611-M-002-003 awarded to KYW.

REFERENCES

Bard, E., 1988: Correlation of accelerator mass spectrometry C-14 ages measured in plank-

- tonic foraminifera: Paleoceanographic implication. *Paleoceanography*, **3**, 635-645.
- Berger, W. H., J. S. Killingly and E. Vincent, 1978: Stable isotopes in deep sea carbonates: Box core ERDC-92, west equatorial Pacific. *Oceanological Acta*, **1**, 203-216.
- Bond, G., W. Broecker, S. Johnsen, J. McManus, L. Labeyrie, J. Jouzel and G. Bonani, 1993: Correlations between climate records from North Atlantic sediments and Greenland ice. *Nature*, **365**, 143-147.
- Broecker, W., 1986: Oxygen isotope constraints on surface ocean temperature. *Quaternary Research*, **26**, 121-134.
- Broecker, W., M. Andree, G. Bonani, W. Wolfli, M. Klas, A. Mix and H. Oeschger, 1988a: Comparison between radiocarbon ages obtained on coexisting planktonic foraminifera. *Paleoceanography*, **3**, 647-657.
- Broecker, W., M. Andree, M. Klas, G. Bonani, W. Wolfli and H. Oeschger, 1988b: New evidence from the South China Sea for an abrupt termination of the last glacial period. *Nature*, **333**, 156-158.
- Broecker, W., 1997: Mountain glaciers: Recorders of atmospheric water content? *Global Biogeochemical Cycles*, **11**, 589-597.
- Cang, S., N. Shackleton, Y. Qin and J. Yan, 1988: The discovery and significance of *Globigerinoides ruber* (pink-pigmented) in Okinawa Trough. *Mar. Geology and Quaternary Geol.*, **8**(1): 24-29. (in Chinese and English).
- Chappell, J. and N.J. Shackleton, 1986: Oxygen isotopes and sea level. *Nature*, **324**, 137-140.
- Chappell, J., A. Omura, T. Esat, M. McCulloch, J. Pandolfi, Ota, Yoko and B. Pillans, 1996: Reconciliation of late Quaternary sea levels derived from coral terraces at Huon Peninsula with deep sea oxygen isotope records. *Earth Planet. Sci. Lett.*, **141**, 227-236.
- Chen, M.T., L. Beaufort and the shipboard scientific party, 1998: Exploring Quaternary variability of the East Asia monsoon, Kuroshio current, and Western Pacific Warm Pool systems: High resolution investigation of paleoceanography from the IMAGES III (MD106) - IPHIS Cruise. *TAO*, **9**, 129-142.
- Chesner, C. A., W. I. Rose, A. Deino, R. Drake and J. A. Westgate, 1991: Eruptive history of Earth's largest Quaternary caldera (Toba, Indonesia) clarified. *Geology*, **19**, 200-203.
- Dansgaard, W., S. J. Johnsen, H. B. Clausen, D. Dahl-Jensen, N. S. Gundestrup, C. H. Hammer, C. S. Hvidberg, J. P. Steffensen, A. E. Sveinbjornsdottir, J. Jouzel and G. Bond, 1993: Evidence for general instability of past climate from a 250-kyr ice-core record. *Nature*, **364**, 218-220.
- DeMenocal, P., Ruddiman, W. and D. Kent, 1990: Depth of p-DRM acquisition in deep-sea sediments - a case study of the B/M reversal and oxygen isotopic stage 19.1. *Earth Planet. Sci. Lett.*, **99**, 1-13.
- Duplessy, J. C., E. Bard, M. Arnold, N. J. Shackleton, J. Duprat and L. Labeyrie, 1991: How fast did the ocean-atmosphere system run during the last deglaciation? *Earth Planet. Sci. Lett.*, **103**, 27-40.
- Fairbanks, R. G., 1989: Glacial-eustatic sea level record 0-17,000 years before present; influence of glacial melting rates on Younger Dryas "event" and deep ocean circulation. *Nature*, **342**, 637-642.
- Fang, X.-M., J.-J. Li, R.V. der Voo, C.M. Niocaill, X.-R. Dai, R.A. Kemp, E. Derbyshire, J.-

- X. Cao, J.-M. Wang and G. Wang, 1997: A record of the Blake event during the last interglacial paleosol in the western Loess Plateau of China. *Earth Planet. Sci. Lett.*, **146**, 73-82.
- Huang, C.Y., P.-M. Liew, M. Zhao, T.-C. Chang, C.-M. Kuo, M.-T. Chen, C.-H. Wang, and L.-F. Zhen, 1997a: Deep sea and lake records of the Southeast Asian paleomonsoons for the last 25 thousand years. *Earth Planet. Sci. Lett.*, **146**, 59-72.
- Huang, C.-Y., S.-F. Wu, M. Zhao, M.-T. Chen, C.-H. Wang, X. Tu and P. B. Yuan, 1997b: Last glacial to interglacial surface ocean variability in the South China Sea: A high-resolution record of sea-surface temperature, productivity, and Southeast Asian monsoon. *Mar. Micropaleontology*, **32**, 71-94.
- Imbrie, J., J. Hay, D. Martinson, A. McIntyre, A. Mix, J. Morley, N. Pisias, W. Prell and N. Shackleton, 1984: The orbital theory of Pleistocene climate: Support from a revised chronology of marine $\delta^{18}\text{O}$ record. In *Milankovitch and Climate*, edited by A. Berger. Reidel, Dordrecht, 269-305pp.
- Linsley, B. K., 1996: Oxygen-isotope record of sea level and climate variations in the Sulu Sea over the past 150,000 years. *Nature*, **380**, 234-237.
- Martinson, D. G., N. Pisias, J. D. Hay, J. Imbrie, T. Moore and N. J. Shackleton, 1987: Age dating and orbital theory of the ice ages: Development of a high-resolution 0 to 300,000-year chronostratigraphy. *Quaternary Res.*, **27**, 1-29.
- Meese, D. A., R. B. Alley, A. J. Gow, P. Grootes, P. A. Mayewski, M. Ram, K. C. Taylor and G. A. Zielinski, 1994: Preliminary depth/age scale of GISP2 core. In: N. H. Hanover (Ed.), *Cold Reg. Res. and Eng. Lab. Spec. Rep.*, 94-1.
- Miao, Q., R. C. Thunell and D. M. Anderson, 1994: Glacial-Holocene carbonate dissolution and sea surface temperature in the South China and Sulu seas. *Paleoceanography*, **9**, 269-290.
- Ninkovich, D., N. J. Shackleton, A. A. Abdel-Monem, J. D. Obradovich and G. Izett, 1978: K-Ar age of late Pleistocene eruption of Toba, north Sumatra. *Nature*, **276**, 574-577.
- Ohkouchi, N., K. Kawamura, T. Nakamura and A. Taira, 1994: Small changes in the sea surface temperature during the last 20,000 years: Molecular evidence from the western tropical Pacific. *Geophysical Research Letter*, **21**(20), 2207-2210.
- Pisias, N. G., D. G. Martinson, T. C. Moore, N. J. Shackleton, W. Prell, J. Hay and G. Boden, 1984: High resolution stratigraphic correlation of benthic oxygen isotopic records spanning the last 300,000 years. *Marine Geology*, **56**, 119-136.
- Prell, W., J. Imbrie, D. G. Martinson, J. J. Morley, N. G. Pisias, N. J. Shackleton and H. F. Streyter, 1986: Graphic correlation of oxygen isotope stratigraphy application to the late Quaternary. *Paleoceanography*, **1**, 137-162.
- Rose, W. I. and C. A. Chesner, 1987: Dispersal of ash in the great Toba eruption, 75 ka. *Geology*, **15**, 913-917.
- Schonfeld, J. and H.-R. Kudrass, 1993: Hemipelagic sediment accumulation rates in the South China Sea related to late Quaternary sea-level changes. *Quaternary Research*, **40**, 368-379.
- Schulz, H., U. von Rad and H. Erlenkeuser, 1998: Correlation between Arabian Sea and Greenland climate oscillations of the past 110,000 years. *Nature*, **393**, 54-57.

- Shackleton, N. J., 1987: Oxygen isotopes, ice volume and sea level. *Quaternary. Sci. Review*, **6**, 183-190.
- Stuiver, M. and P. J. Reimer, 1993: Extend ^{14}C data base and revised CALIB 3.0 ^{14}C age calibration program. *Radiocarbon*, **35**, 215-230.
- Tauxe, L., Herbert, T., Shackleton, N. J. and Y. S. Kok, 1996: Astronomical calibration of the Matuyama-Brunhes boundary: Consequences for magnetic remanence acquisition in marine carbonates and the Asian loess sequences. *Earth Planet. Sci. Lett.*, **140**, 133-146.
- Thompson, P. R., A. W. H. Be, J.-C. Duplessy and N. J. Shackleton, 1979: Disappearance of pink-pigmented *Globigerinoides ruber* at 120,000 yr. BP in the Indian and Pacific Oceans. *Nature*, **280**, 554-558.
- Thunell, R. C., Q. Miao, S. E. Calvert and T. F. Pedersen, 1992: Glacial-Holocene biogenic sedimentation patterns in the South China Sea: Productivity variations and surface water pCO_2 . *Paleoceanography*, **7**, 143-162.
- Thunell, R., D. Anderson, D. Gellar and Q. Miao., 1994: Sea-surface temperature Estimates for the Tropical Western Pacific during the last Glaciation and their Implications for the Pacific Warm Pool. *Quaternary Res.*, **41**, 255-264.
- Thunell, R. C. and Q. Miao, 1996: Sea surface temperature of the western Equatorial Pacific ocean during the Younger Dryas. *Quaternary Res.*, **46**, 72-77.
- Tric, E., C. Laj, J.-P. Valet, P. Tucholka, M. Paterne and F. Guichard, 1991: The Blake geomagnetic event: transition geometry, dynamical characteristics and geomagnetic significance. *Earth Planet. Sci. Lett.*, **102**, 1-13.
- Tucholka, P., M. Fontugne, F. Guichard and M. Paterne, 1987: The Blake magnetic polarity episode in cores from the Mediterranean Sea. *Earth Planet. Sci. Lett.*, **86**, 320-326.
- Wang, C. H., M. P. Chen, S. C. Lo and J. C. Wu, 1986: Stable isotope records of late Pleistocene sediments from the South China Sea. *Bulletin of the Institute of Earth Sciences, Academia Sinica*, **6**, 185-195.
- Wang, C. H. and M. P. Chen, 1990: Upper Pleistocene oxygen and carbon changes of core SCS-15B at the South China Sea. *J. Southeast Asian Earth Sci.*, **4**, 3, 243-246.
- Wang, L. and P. Wang, 1990: Late Quaternary paleoceanography of the South China Sea: Glacial-interglacial contrasts in an enclosed basin. *Paleoceanography*, **5**, 77-90.
- Wang, P., L. Wang, Y. Bian and Z. Jian, 1995: Late Quaternary paleoceanography of the South China Sea: surface circulation and carbonate cycles. *Marine Geology*, **127**, 145-165.
- Wei, K.-Y., M.-Y. Lee, W. Duan, C. Chen and C.-H. Wang, 1998: Paleoceanographic change in the northern South China Sea during the last 15000 years. *J. Quaternary Res.*, **13**, 55-64.
- Wyrtki, K., 1981: An estimate of equatorial upwelling in the Pacific. *J. Physic. Oceanog.*, **11**, 1205-1214.
- Zielinski, G. A., P. A. Mayewski, L. D. Meeker, S. Whitlow and M. S. Twicker, 1996: Potential atmospheric impact of the Toba mega-eruption ~71,000 years ago. *Geophysic. Res. Lett.*, **23**, 837-840.